

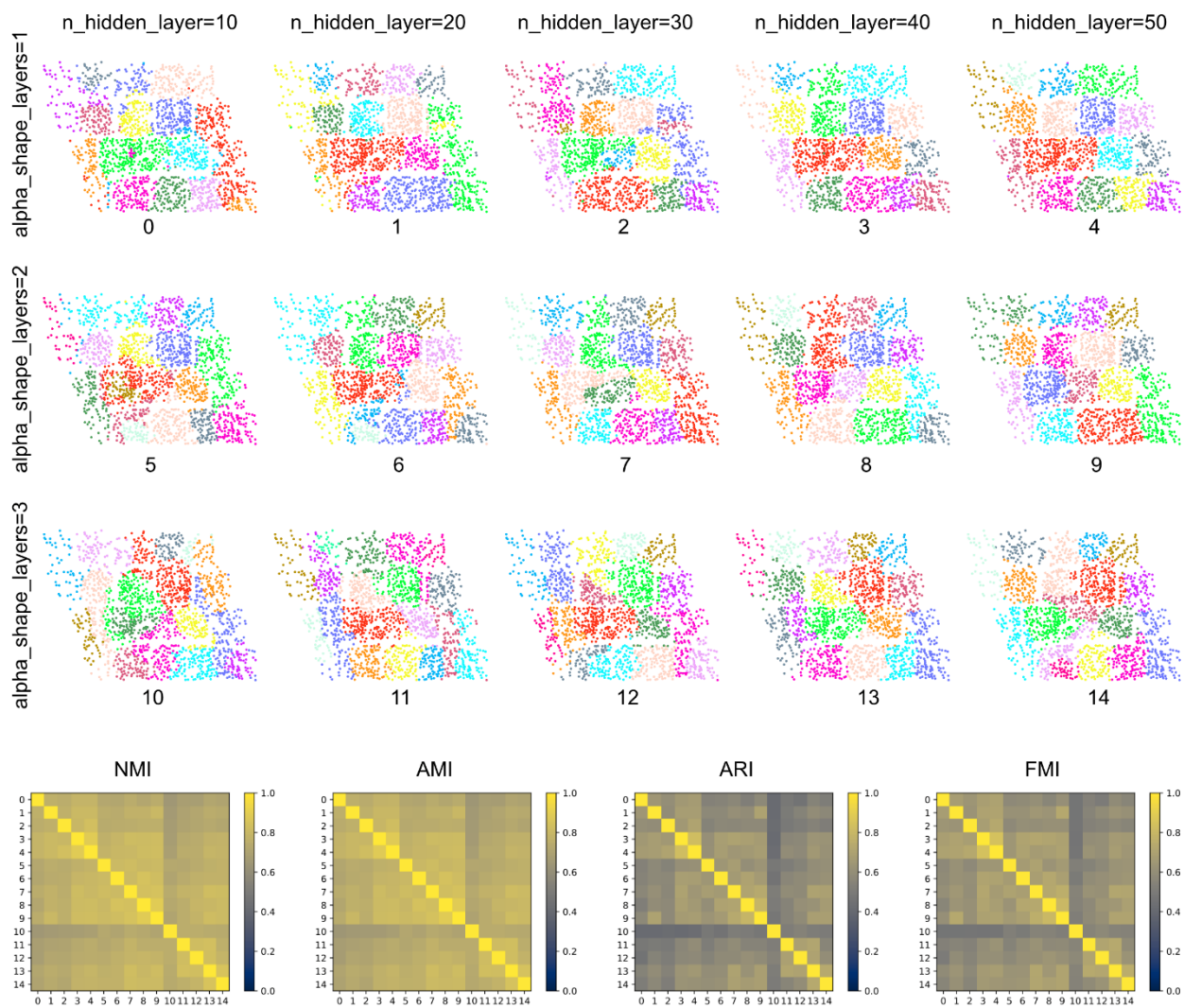
Supplementary Material

Robustness evaluation

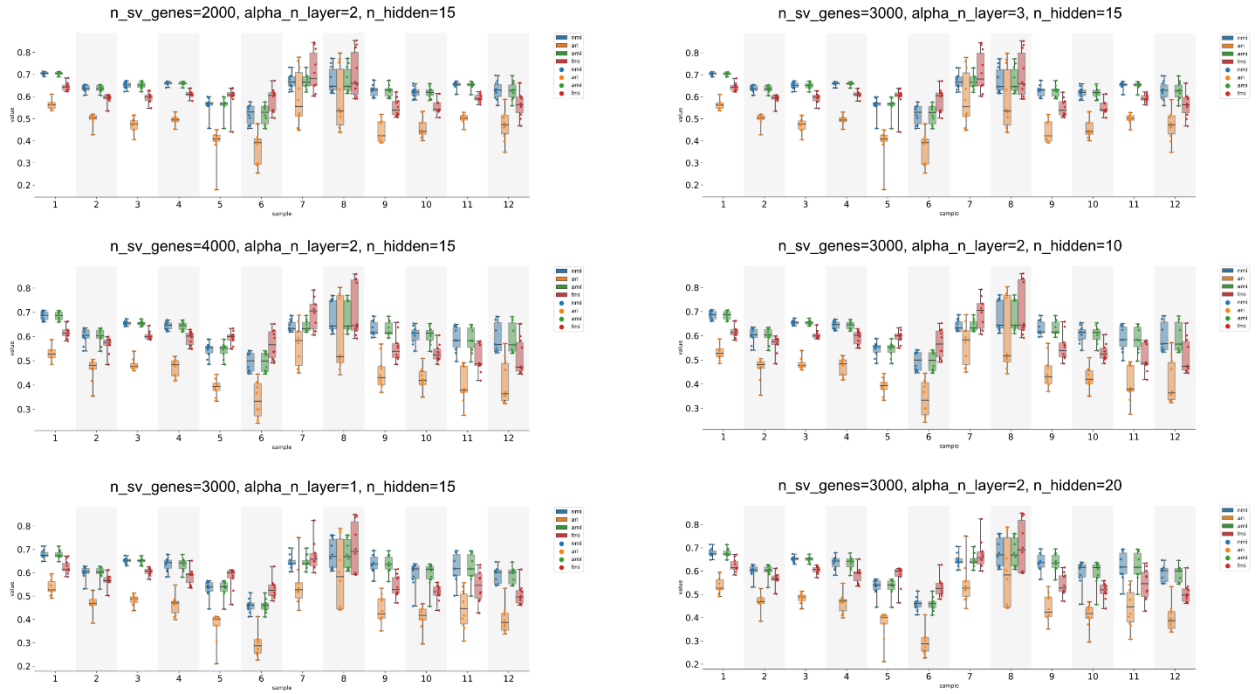
We perturb the key parameters to examine the stability of segmentation results. Two datasets are used, a seqFISH dataset of mouse visual cortex (Zhu et al., 2018) containing 1597 cells and 125 genes, and the benchmark with ground-truth domain segmentation containing 12 Visium datasets of human dorsolateral prefrontal cortex (Maynard et al., 2021). We perturb several key parameters including the number of hidden units (`n_hidden`), the number of layers of the alpha shape based proximity graph (`alpha_shape_layer`), and the number of spatially variable genes used (`n_sv_genes`).

On the seqFISH data, we conducted 15 numerical experiments with different combinations of parameters and compared the segmentation results among the experiments using four standard metrics for clustering, normalized mutual information (NMI), adjusted Rand index (ARI), adjusted mutual information (AMI), and Fowlkes-Mallows index (FMI). Results imply that the segmentation results are highly similar across the numerical experiments (SFigure 1).

On the Visium benchmark datasets, we tested 6 parameter combinations and evaluated the segmentation performance by comparing to the ground-truth using the aforementioned metrics. It was found that our method consistently performs well with all 6 parameter combinations (SFigure 2).



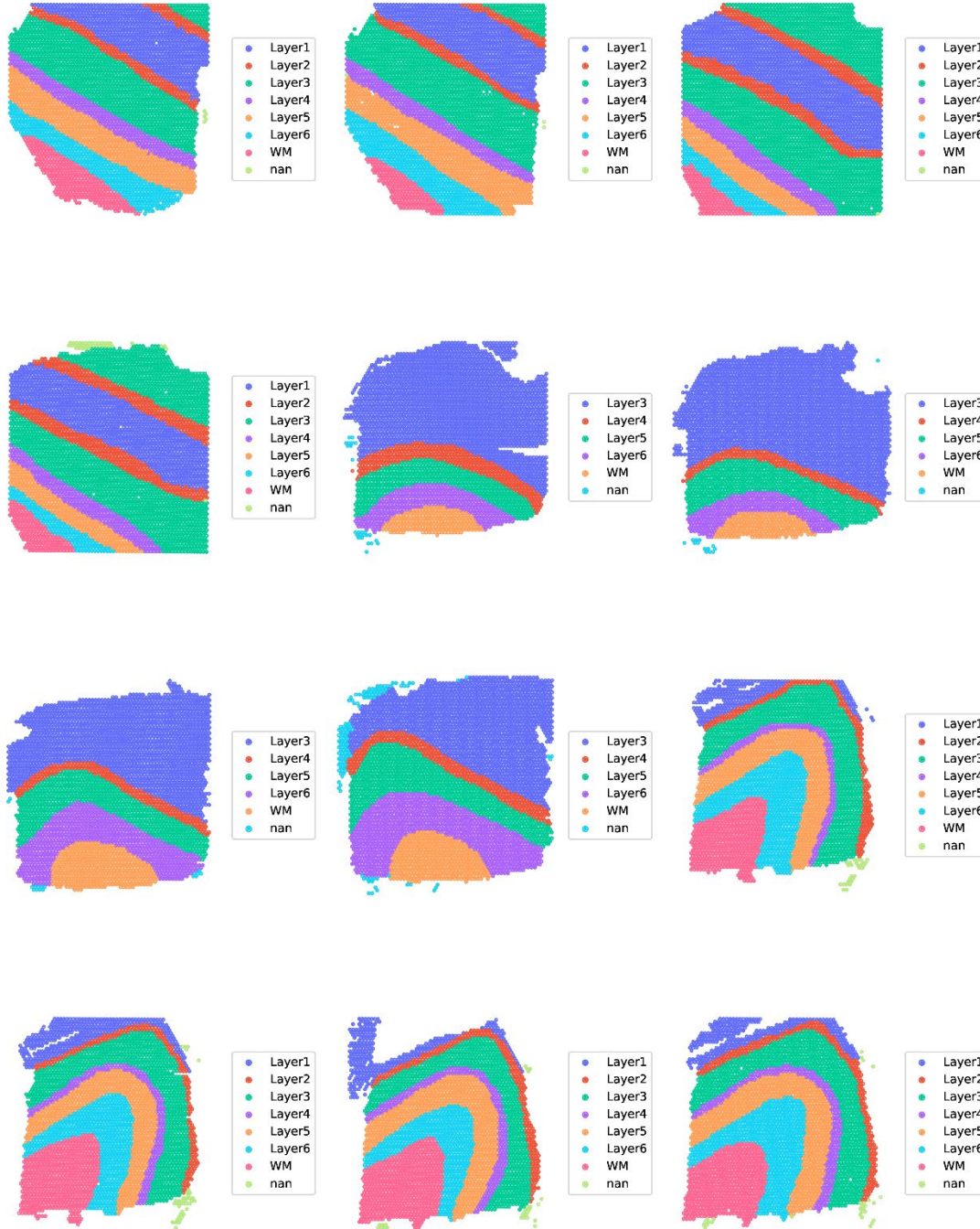
SFigure 1 Robustness of Scan-IT domain segmentation of the seqFISH dataset of mouse visual cortex.



SFigure 2 Robustness of Scan-IT domain segmentation of the benchmark Visium datasets of human dorsolateral prefrontal cortex. To account for randomness, 10 independent runs were carried out for each experiment setup and the results of the parallel runs are shown as box plots.

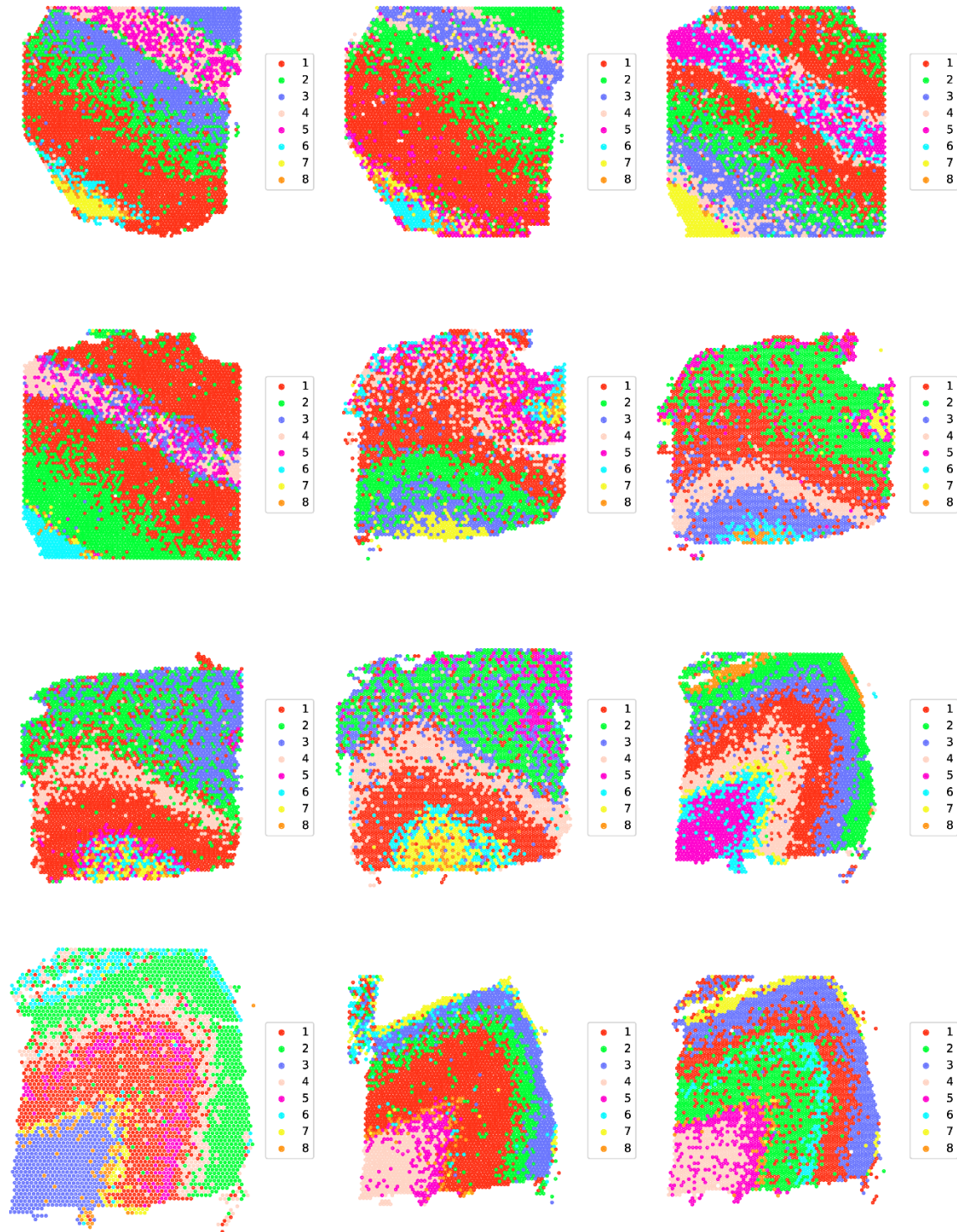
Results of evaluated methods on the Visium benchmark dataset

Ground truth segmentation (Maynard et al., 2021)



SFigure 3 Ground truth domain segmentation of 12 Visium samples of human dorsolateral prefrontal cortex.

SpatialLIBD best parameter combination (Maynard et al., 2021)



SFigure 4 SpatialLIBD segmentation result with the best parameter combinations among the 20 combinations explored in the original publication.

SmfishHmrf segmentation results (Dries et al., 2021; Zhu et al., 2018)

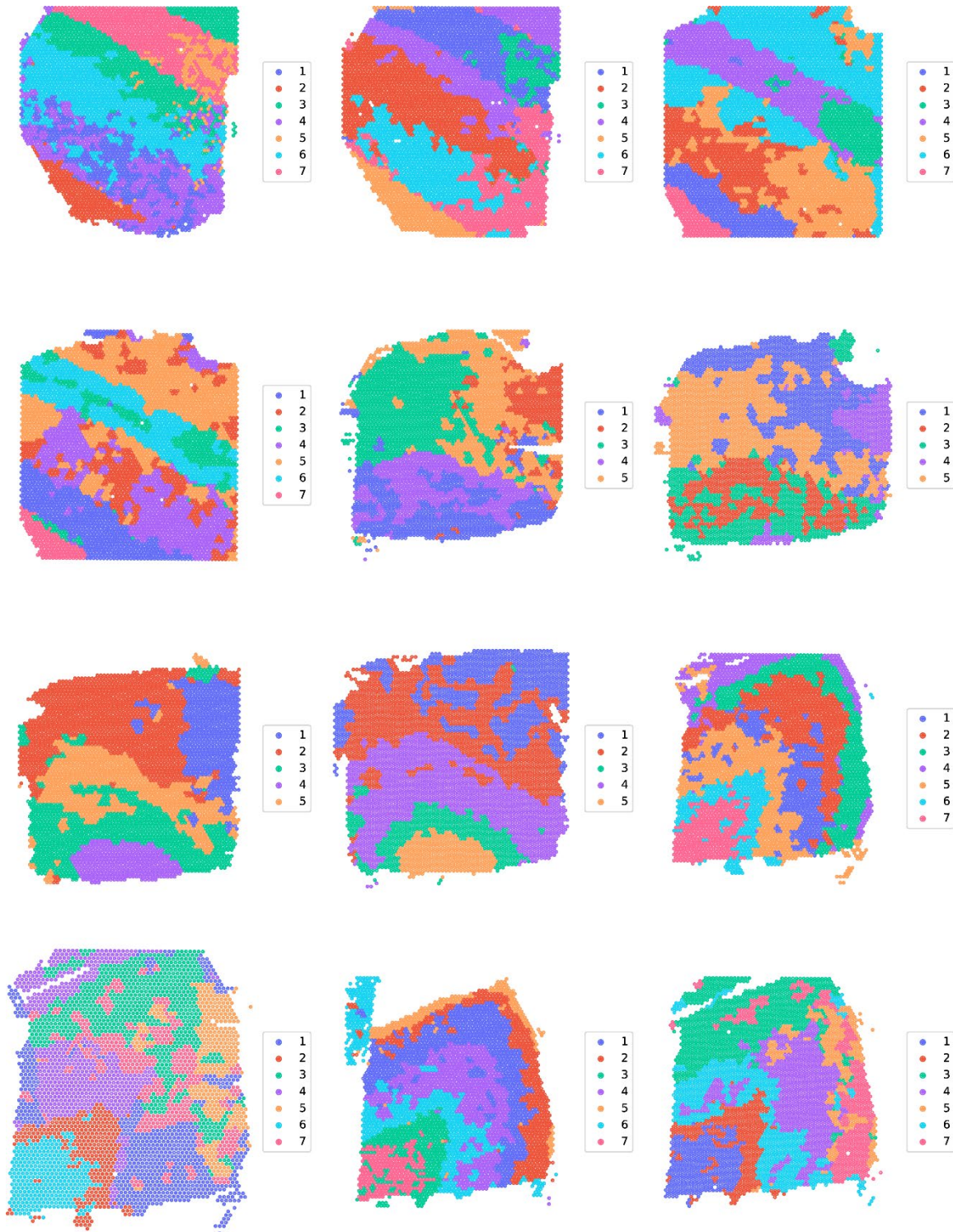


Figure 5 SmfishHmrf segmentation results with the best beta (the key parameter of the model) value 40 among the five tested values, 10, 20, 30, 40, and 50.

StLearn segmentation results (Pham et al., 2020)

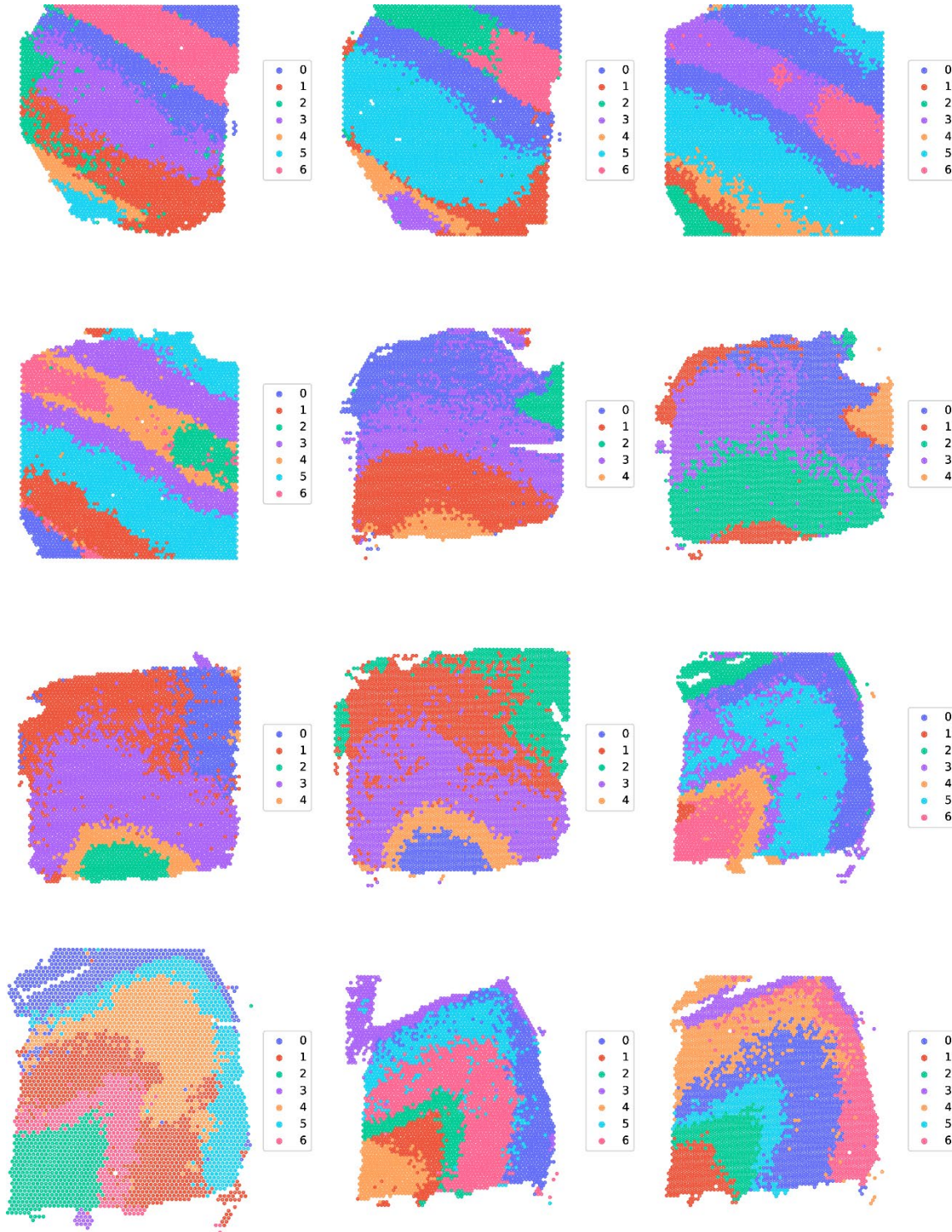
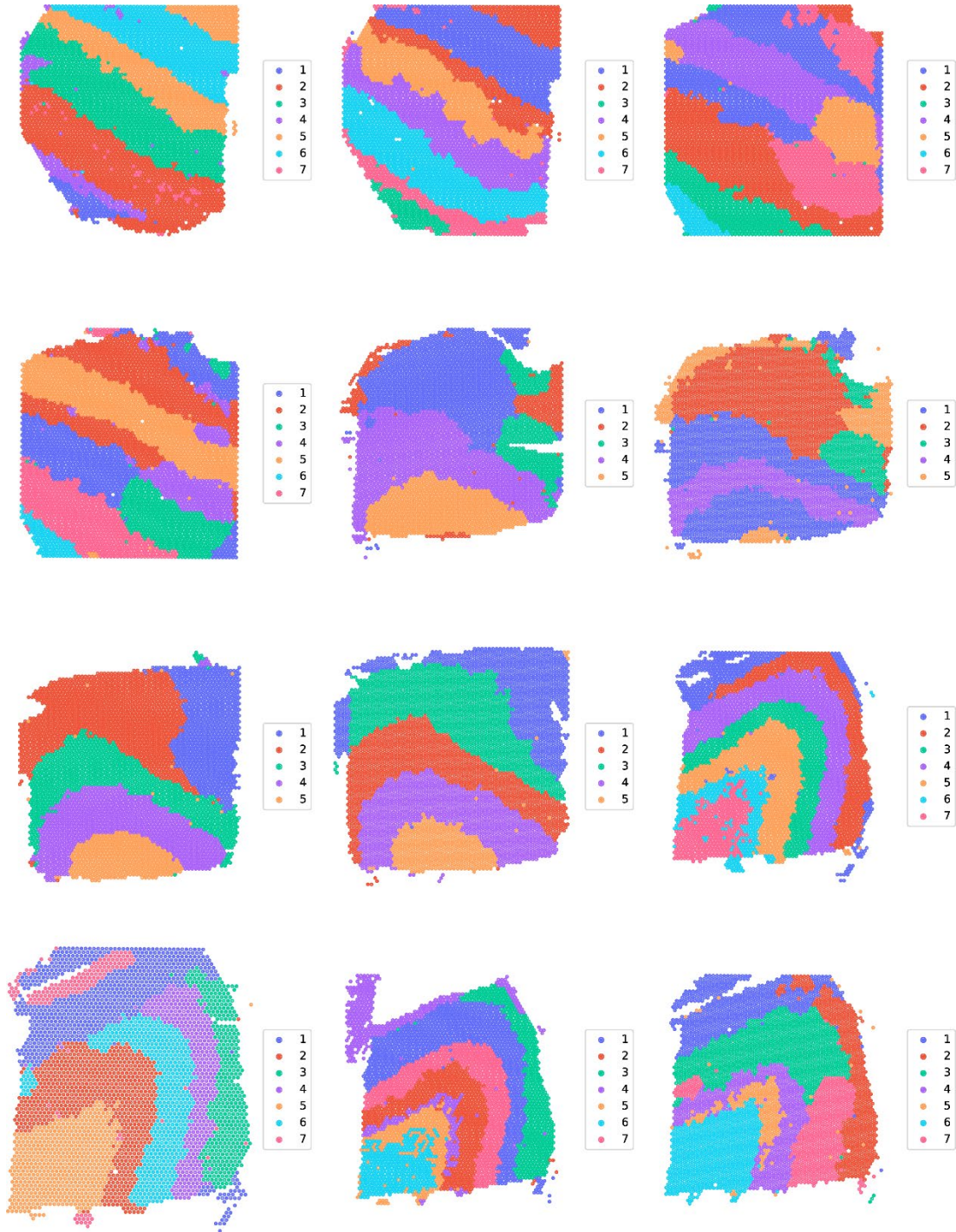


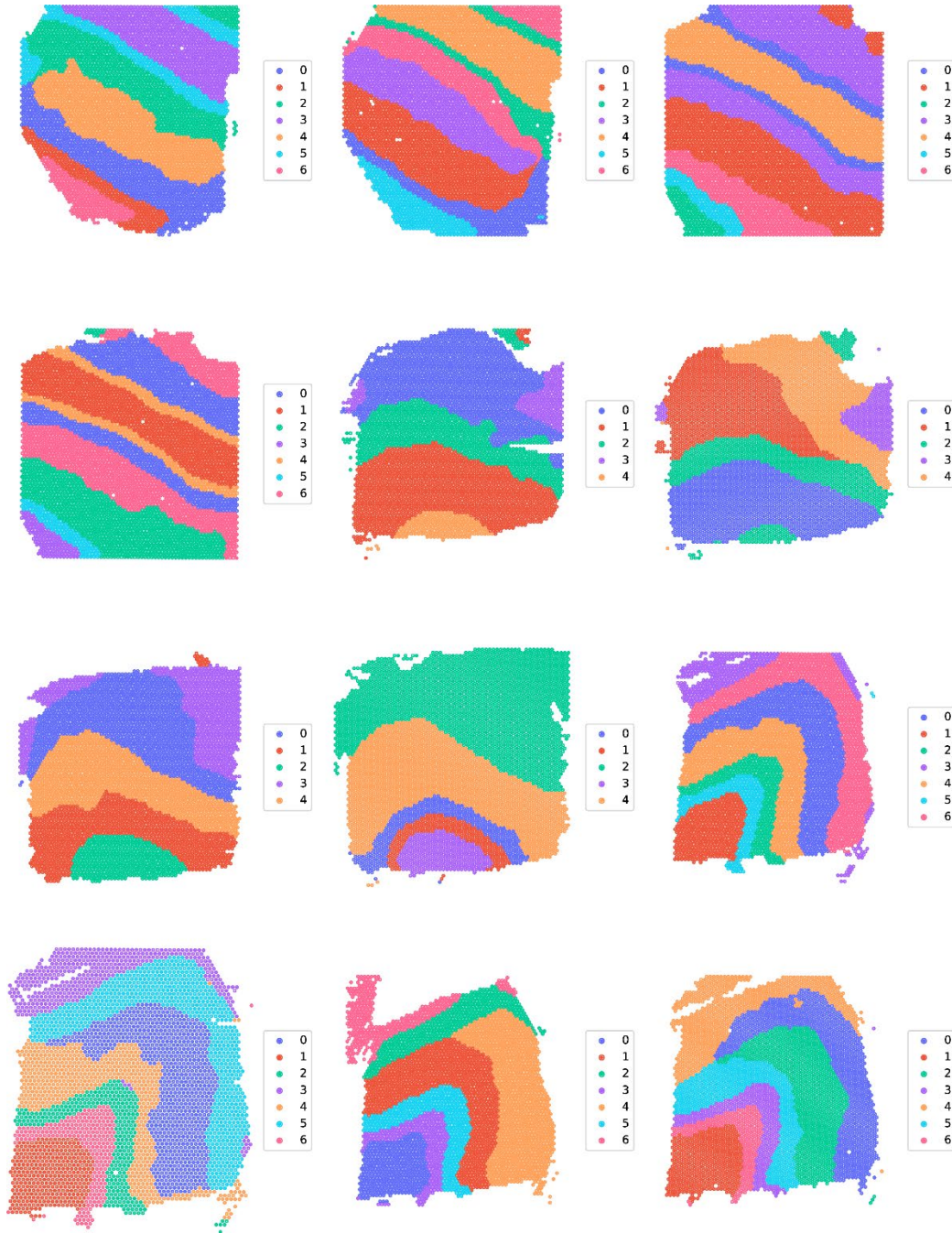
Figure 6 StLearn segmentation results where the result with the median performance among ten independent runs is shown for each of the twelve samples.

BayesSpace segmentation results (Zhao et al., n.d.)



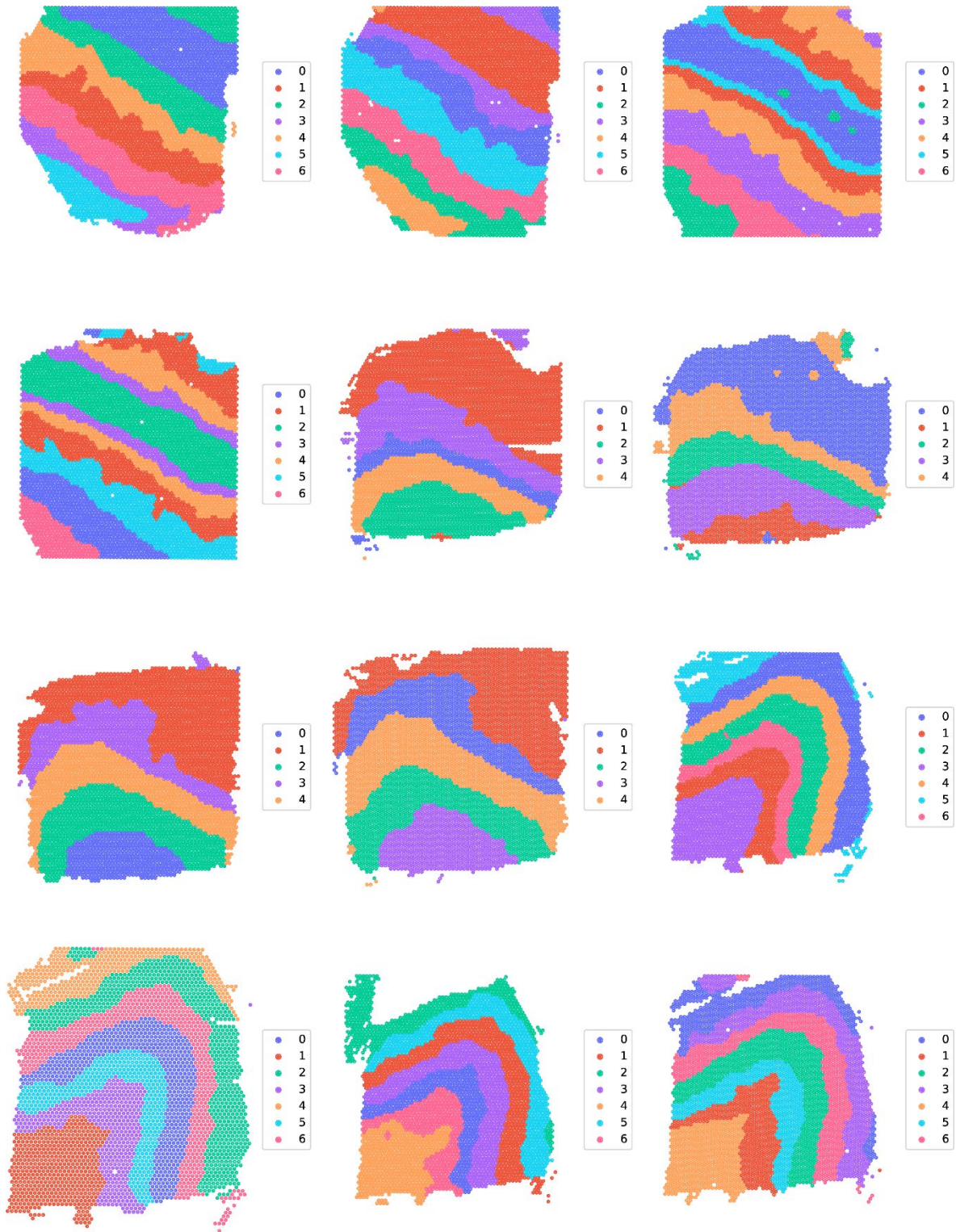
SFigure 7 BayesSpace segmentation results obtained by using the same parameters in the package tutorial.

Scan-IT (SVgenes) segmentation results



SFigure 8 Scan-IT segmentation results using the spatially variable genes determined unbiasedly. The result with the median performance among ten independent runs is shown for each sample.

Scan-IT (markers) segmentation results



*S*Figure 9 Scan-IT segmentation results using the spatial marker genes given in the original publication of the benchmark datasets. The result with the median performance among ten independent runs is shown for each sample.

References

- Dries, R., Zhu, Q., Dong, R., Eng, C.-H. L., Li, H., Liu, K., Fu, Y., Zhao, T., Sarkar, A., Bao, F., George, R. E., Pierson, N., Cai, L., & Yuan, G.-C. (2021). Giotto: a toolbox for integrative analysis and visualization of spatial expression data. *Genome Biology* 22:1, 22(1), 1–31. <https://doi.org/10.1186/S13059-021-02286-2>
- Maynard, K. R., Collado-Torres, L., Weber, L. M., Uytingco, C., Barry, B. K., Williams, S. R., Catallini, J. L., Tran, M. N., Besich, Z., Tippianni, M., Chew, J., Yin, Y., Kleinman, J. E., Hyde, T. M., Rao, N., Hicks, S. C., Martinowich, K., & Jaffe, A. E. (2021). Transcriptome-scale spatial gene expression in the human dorsolateral prefrontal cortex. *Nature Neuroscience*, 24(3), 425–436. <https://doi.org/10.1038/s41593-020-00787-0>
- Pham, D. T., Tan, X., Xu, J., Grice, L. F., Lam, P. Y., Raghubar, A., Vukovic, J., Ruitenberg, M. J., & Nguyen, Q. H. (2020). stLearn: integrating spatial location, tissue morphology and gene expression to find cell types, cell-cell interactions and spatial trajectories within undissociated tissues. *BioRxiv*.
- Zhao, E., Stone, M. R., Ren, X., Pulliam, T., Nghiem, P., Bielas, J. H., & Gottardo, R. (n.d.). *BayesSpace enables the robust characterization of spatial gene expression architecture in tissue sections at increased resolution*. <https://doi.org/10.1101/2020.09.04.283812>
- Zhu, Q., Shah, S., Dries, R., Cai, L., & Yuan, G.-C. (2018). Identification of spatially associated subpopulations by combining scRNAseq and sequential fluorescence in situ hybridization data. *Nature Biotechnology*, 36(12), 1183.